

# On the Numerical Inversion of the Schwarz–Christoffel Conformal Transformation

EUGENIO COSTAMAGNA

**Abstract**—Considering the numerical optimization approach for the inversion of the Schwarz–Christoffel conformal transformation formula, some improvements in integration procedures and some topics in optimization methods are discussed.

Predictor–corrector techniques are introduced in order to map internal lines after the polygonal boundary is transformed; these are applied to the dielectric interface in inhomogeneous line cross sections, allowing conformal transformation of quasi-TEM structures by purely numerical methods. Some examples of computations are presented, and some results are compared to known analytical calculations.

## I. INTRODUCTION

THE SCHWARZ–CHRISTOFFEL (SC) formula, which reads [1]–[3]

$$w(z) = M \int_{z_0}^z \prod_{i=1}^n (\xi - z_i)^{-\mu_i} d\xi + N \quad (1)$$

provides a very general technique for mapping the points on the real axis of the  $z$ -plane upon a polygon in the  $w$ -plane, and the upper half  $z$ -plane to the region enclosed by this polygon. In (1),  $\xi$  is the running variable in the  $z$ -plane, the  $z_i$  ( $i = 1, n$ ) are finite points on the real axis corresponding to the polygon vertices in the  $w$ -plane, and the exponents  $\mu_i$  ( $i = 1, n$ ) are positive or negative real numbers defining the differences in the angular directions of the two consecutive  $w$ -plane sides confluent in the  $w$ , vertex. The constants  $M$  and  $N$  may have complex values, and the lower limit  $z_0$  of the integral may be any point in the upper half plane.

Provided that a suitable algorithm for the inversion of the SC formula is available, very general conformal mapping processes can be performed between different polygonal shapes via an inverse transformation from the original  $w$ -plane to an intermediate  $z$ -plane, and then a direct mapping from this  $z$ -plane to a new  $w'$ -plane, with a new choice of the  $z_i$  points and of the  $\mu_i$  exponents.

As analytical inversion cannot be performed for arbitrary geometries, numerical approaches have been proposed by various authors [3]–[10], resulting in the solution by iterative methods of a set of simultaneous, nonlinear equations relating integrals of the type (1) to the geometrical characteristics of the  $w$ -plane polygon. Several prob-

lems relevant to integration procedures and to optimization schemes have been discussed.

In this contribution, a simple improvement in the application of Gaussian integration formulas is proposed which allows one to cope with very large ratios in the lengths of consecutive  $z$ -plane sides. Some topics in optimization schemes are also discussed. Then, the application of numerical predictor–corrector techniques to the mapping of internal lines is presented, in particular, the mapping of the  $w$ -plane air–dielectric interface of inhomogeneous dielectric, quasi-TEM line structures in the intermediate  $z$ -plane, and then in a new  $w'$ -plane in parallel-plate geometry is discussed. The process can be considered a numerical generalization of the calculations presented in [11] and [12] for inhomogeneous stripline and microstrip line structures. As a result, a transformed rectangular inhomogeneous line cross section is obtained in which, due to the smoothed shape of the new air–dielectric boundary line, successive overrelaxation techniques are very applicable. Examples of the method are discussed in the paper.

## II. INTEGRATION FORMULAS

Various integration procedures have been proposed for the integrals in (1), in particular integration by Simpson's rules with limits displaced from the vertices when these are singular points of the integrand function [4]–[6], integration by Gaussian procedures [7], [8], and by Gaussian procedures with limits displaced from singularities and analytical integration in the remaining part [8]. Gauss–Chebyshev and Gauss–Jacobi quadrature formulas allow singular vertices to be properly considered, and appear to be a very good choice in many cases, as suitable accuracy is provided with short computing times.

The obtainable results can be illustrated by some examples. In the following, formulas 25.4.30, 25.4.37, and 25.4.39 in [13] have been utilized, respectively, for arbitrary intervals and for intervals with  $\mu = 0.5$  vertices at one end or at both ends. Order  $n$  equal to, respectively, 64, 32, and 64 have been considered (i.e., the same zeros of Legendre polynomials and the same weight factors for the 25.4.30 and the 25.4.37 formulas). Gauss–Jacobi quadratures have been performed, computing the  $n$  zeros of the Jacobi polynomials by the routine presented in [14], with  $n = 48$ .

Manuscript received August 13, 1985; revised August 7, 1986.

The author is with Marconi Italiana S.p.A., Genoa, Italy.

IEEE Log Number 8611024.

TABLE I  
RESULTS FOR THE GEOMETRY IN FIG. 1

METHOD OF QUADRATURE	LENGTH OF THE AB AND BC SIDES IN THE w-PLANE AND SIGNIFICANT FIGURE ACCURACY	
	AB	BC
Analytical calculation	1.	
Term-by-term integration (one term retained) + Simpson rule; $a = 1/30$ ; $m = 61$	1.0022	3
As above, but two terms retained	1.000048	5
Gaussian formula ( $n = 32$ )	0.9999999999999991	13

TABLE II  
RESULTS FOR THE GEOMETRY IN FIG. 2

METHOD OF QUADRATURE	LENGTHS OF THE AB AND BC SIDES IN THE w-PLANE AND SIGNIFICANT FIGURE ACCURACIES		
	AB	BC	
Analytical calculation	1.570796326794897	1.831780823064823	
Term-by-term integration (two terms retained) + Simpson rule; $a = 1/30$ ; $m = 61$	1.57088	4	1.8408 2
as above, but $a = 1/100$ , $m = 91$	1.5714	3	1.8338 3
as above, but $a = 1/100$ , $m = 501$	1.5707987	6	1.8324 3
Gaussian formulas ( $n = 32$ and $n = 64$ )	1.570796326794897	16	1.831780823064738 13

In Tables I and II, some data on the accuracy provided by Gaussian formulas for the geometries in Figs. 1 and 2 are shown with reference to analytical calculations. This accuracy compares very favorably with the results provided by Simpson's rule with the number of points specified by the parameter  $m$  and with term-by-term integration near the  $\mu = 0.5$  vertices over the small part of the whole interval specified by the parameter  $a$ .

The geometry in Fig. 2 can be considered as half of a triplate stripline structure: the capacitance and the characteristic impedance can be derived by mapping the  $z$ -axis in Fig. 2 onto a rectangle, after removal of the  $\mu = -1$  vertex at  $z = 0$ . In the usual impedance range of about 50  $\Omega$  (in air), the overall numerical process provides capacitance and impedance values to 12 significant figures with reference to the well-known analytical calculations by elliptic integrals.

In a recent paper [15], a large number of transmission lines formed by regular polygonal coaxial inner and outer conductors have been considered, and the two-dimensional geometrical resistances of the partial regions obtained by dividing the cross section in symmetrical parts have been computed by analytical conformal mapping. The numerical inversion (with the simple optimization procedure described in the next paragraph), followed by a direct transformation into a rectangular geometry has been applied to the same cross sections, utilizing the quoted Gauss-Jacobi procedures to cope with the various  $\mu$  values at the vertices. In all cases [15, figs. 1-6], accuracies of eight to 10 significant figures have been obtained.

Good results have been obtained also by the double

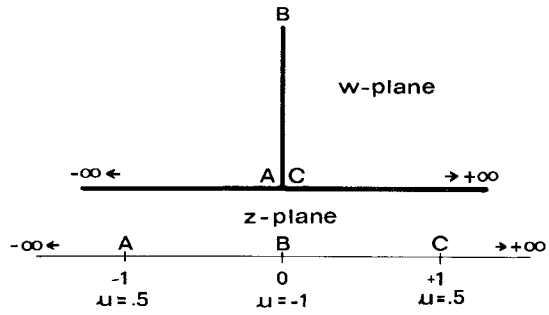


Fig. 1. A simple transformation problem for accuracy tests.

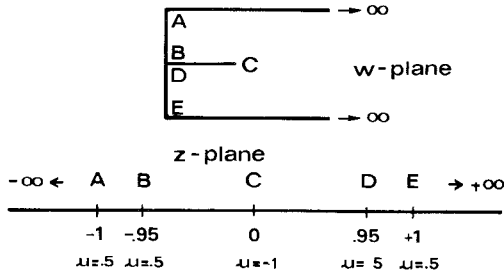


Fig. 2. Transformation problem with five vertices for accuracy tests.

exponential formula [16], although with smaller numbers of significant figures, probably due to a nonoptimized implementation of the algorithm<sup>1</sup>.

In all the preceding examples, values of the order of  $10^2$  or, very seldom,  $10^3$  are not exceeded in the ratios between adjacent sides mapped on the real axis of the  $z$ -plane. Unfortunately, in many practical cases, very large ratios, of the order of  $10^5$  or more, have to be faced during the inversion process, and vertices with positive  $\mu$  can result to be very close to the ends of relatively long sides. This causes severe loss of accuracy, as the Gaussian integration formulas are rather sensitive to the proximity of singular points to the ends of the integration interval. The problem can be illustrated by some representative cases in which numerical computations have been performed by the quoted formulas in [13], and analytical calculations can again provide reference values.

In Fig. 3, some integrand functions are specified by the pertinent sets of  $z_i$  points and  $\mu_i$  exponents and by a sketch of the modulus; the areas corresponding to the integrals to be evaluated are shadowed. Indicating by  $\delta$  the distance of the external singular point from the end of the integration interval, the analytical expressions are:

$$\int_0^{1-\delta} \frac{dz}{\sqrt{1-z}} \quad \text{for type 1} \quad (2)$$

$$\int_0^{1-\delta} \frac{dz}{\sqrt{(z-1)(z-k^2)}}, \quad k^2 = 1 - \delta \quad \text{for type 2} \quad (3)$$

<sup>1</sup>The author wishes to thank an unknown reviewer for pointing out the paramount importance of utilizing in these examples an algorithm well matched to the actual geometries, and for drawing to his attention the study reported in [16].

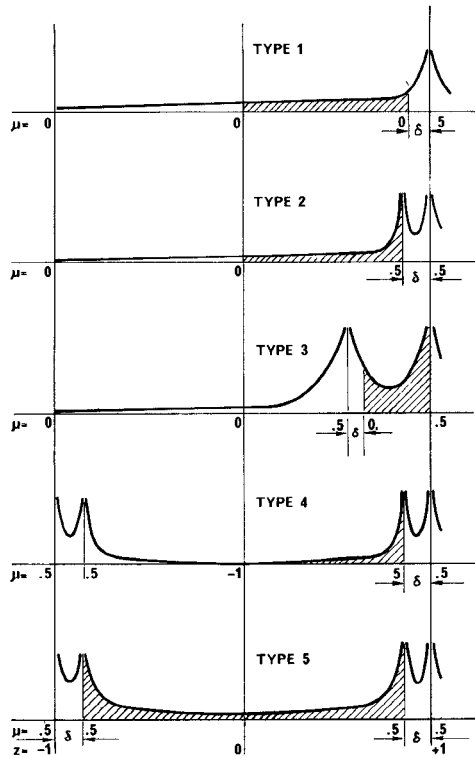


Fig. 3. Some integrals, and the moduli of the integrand functions.

and

$$\int_{k^2 + \delta}^1 \frac{dz}{\sqrt{(z-1)(z-k^2)}}, \quad k^2 = 0.5$$

for type 3 (4)

$$\int_0^{1-\delta} \frac{z dz}{\sqrt{(z^2-1)(z^2-k^2)}}, \quad k = 1 - \delta$$

for type 4 (5)

$$\int_{-1+\delta}^{1-\delta} \frac{dz}{\sqrt{(z^2-1)(z^2-k^2)}}, \quad k = 1 - \delta$$

for type 5. (6)

The errors are plotted in Fig. 4 as a function of the ratio between the distance  $\delta$  and the length  $l$  of the integration interval: when this ratio is smaller than about  $10^{-3}$  or  $10^{-2}$ , depending on the particular function, the relative errors exceed  $10^{-5}$ .

A good solution to this problem has been found by dividing the integration interval in two parts with a suitable length ratio, as shown for a left end in Fig. 5, and performing separate integrations on these parts. The end of the old integration interval, if the corresponding  $\mu$  is positive, becomes an external singular point for the new interval not ending in it (the right-hand side in Fig. 5). Nevertheless, by selecting a length ratio of the order of  $\sqrt{\delta l}/l$ , both the intervals obtained by the partition are allowed a ratio between the distance of the external singular point and the length of the integration interval larger than  $\delta/l$ , and of the order of  $\sqrt{\delta/l}$ .

In the whole range of Fig. 4, accuracies of six to 12

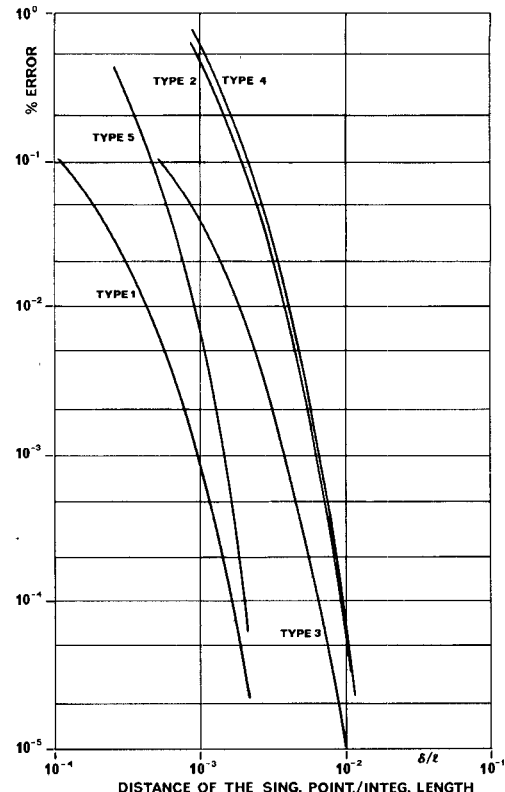


Fig. 4. Percent errors in computing the integrals in Fig. 3 by Gaussian formulas, as a function of the position of an external singular point.

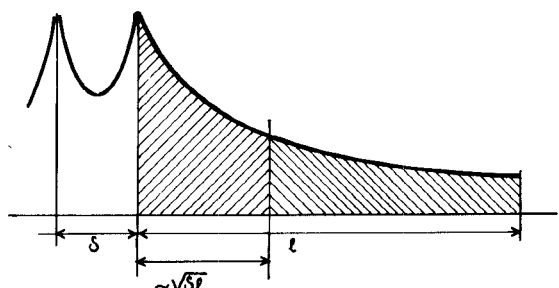


Fig. 5. Partitioning the integration interval.

significant figures have been provided by partitioning the integration interval in this way with partial lengths in a ratio of 1 to 100, and four to six significant figure accuracy by partitioning according to a ratio of 1 to 1000, depending on the type of integral.

Using this technique,  $\delta/l$  ratios of the order of  $10^{-6}$  have been easily handled, and the quadrature procedure is still very fast. For instance, the triplate geometry in Fig. 2 for a characteristic impedance of about  $30 \Omega$  leads to  $z$ -plane ratios of about  $10^3$  to  $10^4$  and to impedance errors, using the simple process, of about 0.5 to 4.5 percent. Using the partition technique, the errors are reduced to less than 0.001 percent.

To cope with greater ratios, partition into three parts has been successfully utilized with partial lengths in a  $1:10^2:10^4$  relationship. Of course, partition is only one of the possible measures: double exponential formulas [16] seem to be very interesting as they lead to clustering of

sampling points near the ends of the integration interval and to a rather insensitive behavior in the presence of singularities close to the ends.

### III. OPTIMIZATION PROCEDURES

Various optimization schemes have been applied to the numerical inversion, including the Powell [6] and Peckham [7] methods, variations of the false position and other simple algorithms for problems with a small number of equations [8], [9], and a modified Hooke and Jeeves method for more difficult cases [10]. In general, direct search strategies have been recommended, as gradient techniques appear to be unsuitable due to difficulties in computing accurate derivatives in the  $w$ -plane.

It is interesting to note that very good results have been obtained in a large number of cases, including the examples discussed in the previous and in the following paragraphs, by a relatively simple algorithm introduced by Maltese [17].

Considering the polygon sides, at any optimization iteration the actual  $z_i - z_{i-1}$  distances are multiplied by the ratios between the wanted and the corresponding actual  $w_i - w_{i-1}$  distances. The process is ended when a simple objective function, obtained by lowering by one the above ratios and summing up the absolute values of the results, is reduced to a specified value or when a new iteration leads to an increased instead than lowered error. The ratios can be raised to some power, normally between 0.5 and 3, to slow or to accelerate convergence. A low exponent normally allows reaching more accurate results and is recommended during the starting iterations. As only information from the corresponding  $w$ -plane side is considered in optimizing any  $z$ -plane side length, the procedure appears to be similar to the one-at-a-time procedure introduced in [3].

The algorithm has been found effective with respect to the accuracy and stability of the results provided by the quadrature routines. No gradient computations are needed and the correct order of the vertices along the real  $z$ -plane axis is implicitly preserved during the process. Invariance of the results within  $10^{-8}$  or better (relative figures) is normally reached after some 50 to a few hundred iterations, and this seems to be of the same order of the number of objective function evaluations reported for more elaborate strategies [6], [7]. In the simple cases considered in [8], accuracies of the same order have been obtained in about 50 iterations in analysis problems.

The partition technique has been proved very useful in rendering the numerical inversion process a general-purpose and reliable design tool, without necessity of excessive care in exploiting any geometrical or physical peculiarity of the actual problem. For instance, no diligence is needed in avoiding unnecessarily high ratios in the  $w$ -plane side lengths, nor in performing residue evaluations in the case of  $w$ -plane sides meeting at infinity [3]. A favorable choice of the relative positions of the transformed vertices along the real  $z$ -plane axis can be very important. In some cases [2], as in the conformal transformation of polygons without vertices at infinity, after the relative positions have been settled, three  $z$ -plane points (i.e., a third point in

addition to  $z_1$  and  $z_n$ , which are normally placed at the  $-1$  and  $+1$  normalized abscissas) can still be chosen to correspond to an arbitrary  $w$ -plane polygon boundary point. This possibility has been proved useful in order to avoid clustering of  $z$ -plane vertices, thereby reducing accuracy problems.

The numerical optimization processes, due to the computer time and to the inherent complexity, are more useful in cases where no simpler computing methods are available. This means that no simple ways to ascertain the obtained accuracy are available. Therefore, it is advisable when possible to perform the inverse transformation starting from different conditions and to compare the results.

### IV. MAPPING $w$ -PLANE PATTERNS

When the positions of the  $z_i$  points have been determined by the inversion procedure, any  $w$ -plane pattern can be mapped into the  $z$ -plane. In particular, internal lines of the original polygon can be mapped by applying in the complex plane the techniques described in [18] (and something similar was foreshadowed in [3]). The problem can be described by the equation

$$\frac{\Delta z}{\Delta w} = \frac{1}{F(z)} \quad (7)$$

where  $\Delta z$  and  $\Delta w$  are the corresponding  $z$ -plane and  $w$ -plane displacements, and  $F(z)$  is the integrand function in (1).

A single-step predictor-corrector method has been utilized. At the step  $k$ , the new  $z$ -plane position  $\bar{z}_{k+1}$  is predicted by the Euler algorithm

$$\bar{z}_{k+1} = \bar{z}_k + \Delta w \frac{1}{F(\bar{z}_k)} \quad (8)$$

and corrected by the Heun algorithm

$$\bar{z}_{k+1} = \bar{z}_k + \frac{\Delta w}{2} \left[ \frac{1}{F(\bar{z}_k)} + \frac{1}{F(\bar{z}_{k+1})} \right]. \quad (9)$$

A correction loop of no more than five iterations has been shown adequate. In simple cases, no large differences have been found in the results of two to 10 iteration loops. The number of steps was more important, and in some cases the error in the position of the final point has been lowered by more than an order of magnitude by changing from 100 to 500 steps.

The mapping procedure can be started from any  $w$ -plane point, provided that the position of the corresponding  $z$ -plane point is given. When the  $w$ -plane starting point lies on a side of the polygon, this position has been determined by standard Newton-Raphson or bisection techniques, performing length calculations by the Gaussian quadrature routines. Starting from a polygon vertex (with  $0 < \mu < 1$ ), the first  $\Delta z$  has been determined by considering the Guillemin's series representation of (1) [1], and retaining the first-order term.

When remapping the obtained  $z$ -plane pattern into a new  $w'$ -plane, the Heun algorithm can be simply applied as the next  $z$ -plane point is already known in this case.

In many cases derived from simple stripline and microstrip geometries, in particular in mapping air-dielectric interfaces, the positional errors in the  $z$ -plane or  $w'$ -plane pattern ending points have been of the order of  $10^{-3}$  or  $10^{-2}$  with respect to the total pattern length. In the case of more complicated geometries, e.g., coupled microstrips or similar, typical results have shown errors in length and in direction in the last part of the  $z$ -plane and  $w'$ -plane patterns when the aimed end point was a  $z$ -plane singular point. In many cases, however, the companion maps obtained starting from the opposite ends of a given  $w$ -plane pattern have shown good overlapping, even if no perfect point-to-point agreement was obtained.

The numerical mapping of internal lines seems to be very dependent on accurate positioning of the  $z$ -plane vertices: as typical consequence of high ratios between the lengths of consecutive  $z$ -plane sides, superimposed  $w$ -plane patterns starting from opposite ends can result in "parallel"  $w'$ -plane maps, and partition of the integration interval in three parts (a singular point very close to one end) or in five parts (two singular points very close to both ends) has sometimes been necessary to recover good pattern coincidence.

In conclusion, as the examples will show, the numerical mapping techniques seem to be highly suitable for interactive computer-aided design operations, although not suitable for fully automatic procedures.

## V. INHOMOGENEOUS DIELECTRIC EXAMPLES

Mapping dielectric interfaces together with the outer boundary in a parallel-plate configuration normally leads to smoothed inhomogeneous line structures in which discrete approximation methods and in particular successive overrelaxation (SOR) techniques can provide accurate evaluations of the quasi-TEM characteristics with limited computation effort. This has been done by analytical interface mapping in [11] and [12], and can be performed by a purely numerical procedure when analytical methods are not available.

The six to seven figure characteristic impedance and effective permittivity data presented in [12, tables II and III] permit an appreciation of the accuracy of the results obtained for the same microstrip line structures by predictor-corrector techniques followed by SOR procedures [19] based on square grids of about  $100 \times 70$  to  $100 \times 20$  nodal points. The quoted tables refer to different values of the relative permittivity  $\epsilon_r$ . In the whole considered range of line dimensions (except in the last two cases, related to very large strips), differences in impedance values of about 0.1 to 0.4 percent with differences in effective relative permittivity of about 0.2 to 0.6 percent have been obtained for  $\epsilon_r = 4.2$ , and differences in impedance values of about 0.2 to 0.8 percent with differences in effective relative permittivity of about 0.5 to 1.7 percent have been obtained for  $\epsilon_r = 51$ : the results of the whole process seem to be well suited for computer-aided design purposes.

The inhomogeneous dielectric coplanar waveguide with lower ground plane can provide further examples. No exact calculations are known for this structure, but some

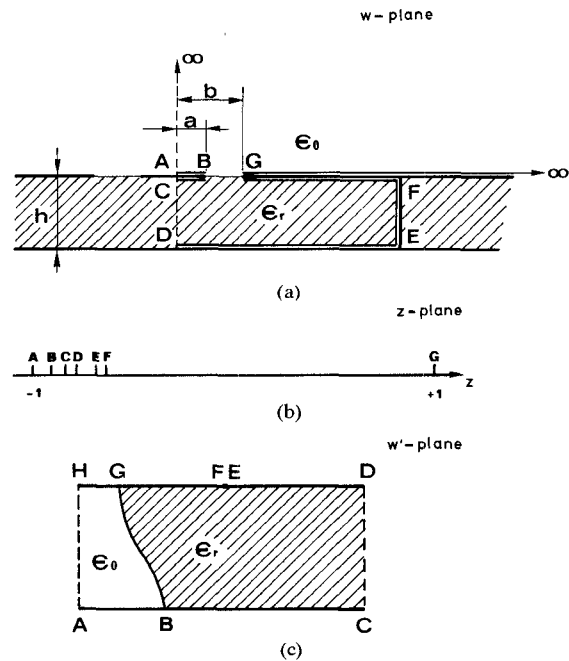


Fig. 6. A coplanar waveguide with lower ground plane structure in inhomogeneous dielectric, and a related inverse SC transformation problem.

results derived in [20] by a very good approximate conformal mapping technique leading to analytical computations can supply comparison data. The structure is shown in Fig. 6(a) where the geometry considered for the numerical conformal mapping is superimposed. Continuous lines indicate electric walls, dotted lines magnetic walls.

In [20] a magnetic wall was assumed at the air-dielectric interface. In the present calculations this approximation has been avoided, and the geometry of Fig. 6(a) first mapped via the optimization technique into the  $z$ -plane of Fig. 6(b), and then by direct SC transformation into the rectangular geometry of Fig. 6(c).

Sufficient distance between the vertices  $F$  and  $G$  to obtain a negligible distance between the points in the  $w'$ -plane corresponding to the vertices  $E$  and  $F$  (negligible dielectric flux on the  $EF$  side) has been assumed, and square grids of about  $100 \times 80$  to  $100 \times 20$  nodal points have been adopted in the SOR process. Some final results for characteristic impedances and effective relative permittivities are shown in Figs. 7 and 8, together with reference curves derived from the results published in [20] (the substrate permittivity is  $\epsilon_r = 10$ ): the agreement between the results provided by the different computation techniques is very good. Only in the region of large gaps and thin substrates are some discrepancies noticeable, especially in the effective permittivities, probably due to some deficiency of the magnetic wall assumption in [20].

It should be noted that in some cases (low right side in Fig. 7) partition techniques in the Gaussian integration have been necessary due to the relatively wide inner strip, and in many cases if partition techniques are not adopted considerable care is necessary in selecting a  $w$ -plane  $FG$  distance suitable for obtaining negligible dielectric flux on the  $EF$  side and still secure sufficiently low  $z$ -plane side

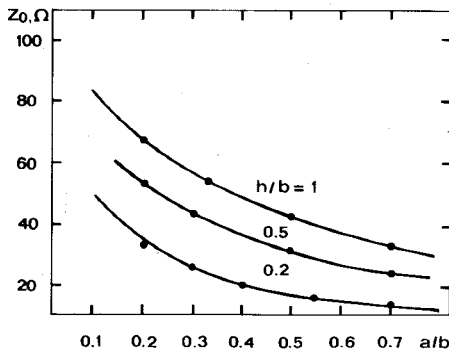


Fig. 7. Some results from numerical inversion of the SC transformation for the characteristic impedance of the structure in Fig. 6, shown as dots and compared with curves derived from [20].

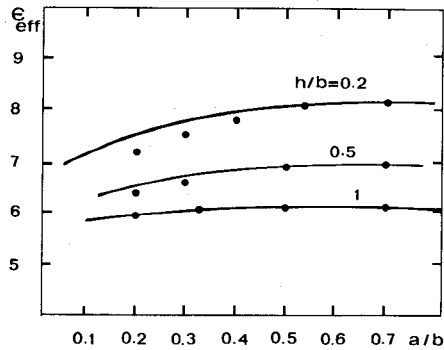


Fig. 8. Some results from numerical inversion of the SC transformation for the effective relative permittivity of the structure in Fig. 6, shown as dots and compared with curves derived from [20].

ratios. Partition techniques on the other hand lead in any case to good  $w'$ -plane dimensions and mapped interface patterns without any care in  $w'$ -plane dimension selection.

## VI. CONCLUSIONS

Numerical optimization methods for the inversion of the Schwarz-Christoffel formula have been considered, and simple interval partition techniques have been suggested to cope with singular vertices very close to the ends of any integration interval in the transformed real axis. Such vertices have been recognized as a major cause of inaccurate results with traditional quadrature procedures.

Numerical predictor-corrector techniques have been proposed for line mapping, and some examples of transformation of the dielectric interface and evaluation of the quasi-TEM characteristics in inhomogeneous structures have been discussed.

Partition techniques, simple optimization procedures, and numerical mapping of dielectric interfaces allow conformal transformations of inhomogeneous transmission line geometries with accuracy suitable for computer-aided design and acceptable operator skill.

## ACKNOWLEDGMENT

The author is indebted to U. Maltese, who suggested this research and introduced the optimization algorithm implementing the first computer trial program, based on series development two-term integration procedures. Initial work on this contribution including quadrature by stan-

dard Gaussian formulas was performed by Maltese and the author in 1970-1971. Very useful observations on the argument by Dr. S. B. Cohn and very valuable suggestions by the reviewers of the manuscript are gratefully acknowledged. The author wishes to thank the Technical Director of Marconi Italiana for permission to publish this paper.

## REFERENCES

- [1] E. A. Guillemin, *The Mathematics of Circuit Analysis*. New York: Wiley, 1950, ch. VI, art. 25.
- [2] E. Durand, *Électrostatique*, tome II. Paris: Masson et Cie., 1964, Ch. IV, part IX.
- [3] K. J. Binns and P. J. Lawrenson, *Analysis and Computation of Electric and Magnetic Field Problems*. New York: Pergamon Press, 1963, paragraphs 8.2 and 10.5.
- [4] K. J. Binns, "The magnetic field and centering force of displaced ventilating ducts in machine cores," *Proc. Inst. Elec. Eng.*, vol. 108, pt. C, pp. 64-70, 1961.
- [5] K. J. Binns, "Calculation of some basic flux quantities in induction and other doubly-slotted electrical machines," *Proc. Inst. Elec. Eng.*, vol. 111, no. 11, pp. 1847-1858, Nov. 1964.
- [6] P. J. Lawrenson and S. K. Gupta, "Conformal transformation employing direct-search techniques of minimization," *Proc. Inst. Elec. Eng.*, vol. 115, no. 3, pp. 427-431, Mar. 1968.
- [7] D. Howe, "The application of numerical methods to the conformal transformation of polygonal boundaries," *J. Inst. Math. Appl.*, vol. 12, pp. 125-136, 1973.
- [8] K. Foster and R. Anderson, "Transmission-line properties by conformal mapping," *Proc. Inst. Elec. Eng.*, vol. 121, no. 5, pp. 337-339, May 1974.
- [9] R. Anderson, "Analogue-numerical approach to conformal mapping," *Proc. Inst. Elec. Eng.*, vol. 122, no. 9, pp. 874-876, Sept. 1975.
- [10] K. J. Binns and G. Rowlands Rees, "Analogue-numerical approach to conformal mapping" (comments on the paper in [9], and reply by R. Anderson), *Proc. Inst. Elec. Eng.*, vol. 123, no. 3, p. 212, Mar. 1976.
- [11] K. K. Joshi, J. S. Rao, and B. N. Das, "Analysis of inhomogeneously filled stripline and microstripline," *Proc. Inst. Elec. Eng.*, vol. 127, pt. H, no. 1, pp. 11-14, Feb. 1980.
- [12] R. C. Callarotti and A. Gallo, "On the solution of a microstripline with two dielectrics," *IEEE Trans. Microwave Theory Tech.*, vol. MTT-32, no. 4, pp. 333-339, Apr. 1984.
- [13] M. Abramowitz and I. A. Stegun, Eds., *Handbook of Mathematical Functions*. New York: Dover, 1965, pp. 887-889.
- [14] A. H. Stroud and D. Secrest, *Gaussian Quadrature Formulas*. Englewood Cliffs, NJ: Prentice-Hall, 1966, sections 2.2 and 2.5.
- [15] R. Terakado, "Exact wave resistance of coaxial regular polygonal conductors," *IEEE Trans. Microwave Theory Tech.*, vol. MTT-33, pp. 143-145, Feb. 1985.
- [16] H. Takahasi and M. Mori, "Double exponential formulas for numerical integration," *Publ. R.I.M.S.*, Kyoto Univ., no. 9, pp. 721-741, 1974.
- [17] U. Maltese, unpublished work and FORTRAN program, Marconi Italiana S.p.A., 1970-1971.
- [18] L. O. Chua, "Computer-aided analysis of nonlinear networks," in *Computer-Oriented Circuit Design*, F. F. Kuo and W. G. Magnuson, Jr., Eds. Englewood Cliffs, NJ: Prentice-Hall, 1960, pp. 166-171.
- [19] H. E. Green, "The numerical solution of some important transmission-line problems," *IEEE Trans. Microwave Theory Tech.*, vol. MTT-13, no. 5, pp. 676-692, Sept. 1965.
- [20] G. Ghione and C. Naldi, "Parameters of coplanar waveguides with lower ground plane," *Electron. Lett.*, vol. 19, no. 18, pp. 734-735, Sept. 1983.



Eugenio Costamagna was born in Genoa, Italy, on June 26, 1942. He received the dott. ing. degree in electronic engineering from the University of Genoa, Italy, in 1967.



Since 1967, he has been with Marconi Italiana in Genoa, where he is involved in communication circuit and system design and in related computer-oriented techniques. His main interests are in the fields of distributed networks, in particular using microstrip, mechanical filters, and monolithic crystal devices, and in numerical simulation techniques for transmission devices and systems.